Natural orbitals, overlap functions, and mean-field orbitals in an exactly solvable A-body system

D. Van Neck and A. E. L. Dieperink
Kernfysisch Versneller Instituut, Zernikelaan 25, 9747 AA Groningen, The Netherlands

M. Waroquier
Laboratory for Theoretical Physics, Proeftuinstraat 86, B-9000 Gent, Belgium

(Received 30 November 1995)

We consider a simple but nontrivial many-body system interacting through short-range forces, and confirm a property of such systems that was recently proposed on general grounds, namely, that single-particle overlap functions, spectroscopic factors, and separation energies of the bound $(A-1)$-particle eigenstates can be derived from the one-body density matrix of the A-particle system in its ground state. The basis of natural orbitals for the system is constructed and its properties are discussed. We also investigate the high-momentum content of the bound-state overlap functions and momentum distribution. It is found that the mean field provides a good approximation for the bound-state overlap functions even in the region of large momenta, where the total momentum distribution is already enhanced by several orders of magnitude over the mean-field result.

PACS number(s): 24.10.Cn, 21.60.−n, 21.10.Pc

I. INTRODUCTION

Correlations play a central role in the description of the nuclear wave function for large momenta $k>k_F$. These high-momentum components are of interest as they involve the short-range dynamics of a nucleon-nucleon (NN) pair in the nuclear medium.

In this context the influence of NN correlations on single-particle quantities is of particular importance, since these are the most easily accessible through experiment. One-nucleon knockout reactions like $(e,e'p)$, for example, are sensitive to the one-body spectral function [1], although the interpretation is complicated by large distorting effects such as final-state interactions and mesonic exchange currents.

Ideally one could look for effects of NN correlations in $(e,e'p)$ reactions at missing energies beyond the threshold for two-nucleon emission, but in practice most experiments up to now were limited to small missing energies, where the residual $(A-1)$ system is left in a discrete bound state. It was shown recently [2] that in a perturbative Green function approach for a finite system like ^{16}O the overlap function leading to a bound $(A-1)$ eigenstate has no appreciable enhancement of high-momentum components (at least up to 600 MeV/c) when compared to a typical mean-field calculation. In [3] we pointed out that the spectral function in the local density approximation (LDA) is consistent with this result. In this paper we will demonstrate that an exactly solvable schematic model exhibits the same feature as found in these calculations, namely, that at small values of the removal energy the spectral function is well approximated by the mean-field result, even at large momentum.

In a previous paper by the authors [4] it has been shown that some quantities related to the $(A-1)$-particle system [such as separation energies, spectroscopic factors, and overlap functions for the bound $(A-1)$ states] are fully determined by the one-body density matrix (OBDM) of the A-particle system in its ground state. This surprising theorem holds quite generally for quantum many-body systems interacting through forces of sufficiently short range. Essential in the derivation of the theorem is the assumption that the convergence (to their exponential asymptotic regime) of the overlap functions in the decomposition of the OBDM is uniform. Since this is not clear *a priori* it is of some interest to introduce a schematic model in which all single-particle quantities can be calculated exactly.

An example of such a model, being both exactly solvable and containing the relevant many-body correlations, consists of a system of spinless particles in one dimension interacting through delta function two-body potentials (see, e.g., [5,6]). It has been applied previously to the problem of nuclear form factors and momentum distributions [7–9]. The aim of this paper is then twofold. First, we want to check explicitly in this model the general results obtained in [4]. To this end we construct the full OBDM which, to the best of our knowledge, has not been obtained before for this model. Second, we study the contribution of the bound $(A-1)$ eigenstates to the momentum distribution and discuss the high-momentum behavior of this contribution and of the total momentum distribution.

The remainder of this paper is organized as follows. The schematic model that we solve is outlined in Sec. II. In Sec. III we construct the OBDM and study its asymptotic behavior in coordinate space and its relation to the overlap functions. In Sec. IV the high-momentum components in the momentum distribution and the bound-state overlap functions are investigated. Section V contains a summary and conclusions. The definitions and conventions for the various single-particle quantities are gathered in Appendix A.

II. ONE-DIMENSIONAL MODEL

The model we will discuss involves A spinless bosons moving in one dimension and interacting through attractive δ-function potentials. The corresponding Hamiltonian is

$$H=-\frac{1}{2m}\sum_{i=1}^{A}\frac{\partial^2}{\partial x_i^2}-g\sum_{i<j=1}^{A}\delta(x_i-x_j), \tag{1}$$

with $g>0$ and in units $\hbar=1$. We summarize briefly some previous results that have been obtained for this system.

For all $A\geqslant 2$ there is just one bound state with energy

$$E_{0(A)}=-\frac{1}{24}mg^2A(A^2-1) \tag{2}$$

and with intrinsic wave function ($\lambda=mg/2$)

$$\Psi_A(x_1,\ldots,x_A)=C_A\exp\left(-\lambda\sum_{i<j=1}^{A}|x_i-x_j|\right). \tag{3}$$

In Eq. (3) the normalization constant is given by $C_A=[(2\lambda)^{A-1}(A-1)!/A]^{1/2}$. We refer to Appendix A for our normalization conventions.

The above model was studied by Calogero and Degasperis [6], who obtained a closed-form expression for the one-body density [see Eq. (A13)],

$$\rho(y)=2\lambda A(A-1)\sum_{n=1}^{A-1}nF_n^{(A)}e^{-2n\lambda(A-1)|y|} \tag{4}$$

and hence also (by Fourier transforming) for the form factor. The coefficients $F_n^{(A)}$ in Eq. (4) are given by the combinatorial expression

$$F_n^{(A)}=(-1)^{n+1}\frac{[(A-1)!]^2}{(A-1-n)!(A-1+n)!}. \tag{5}$$

The mean-field (Hartree) approximation for this model was also derived analytically by Calogero and Degasperis [6]. The Hartree solution is $\Psi_A(x_1,\ldots,x_A)=\Pi_{i=1}^{A}\varphi_A(x_i)$, with the single-particle wave function given by

$$\varphi_A(x)=\sqrt{\frac{\lambda A}{2}}\frac{1}{\cosh(\lambda Ax)}. \tag{6}$$

The Hartree approximation for the one-body density is then

$$\rho^H(y)=A|\varphi_A(y)|^2. \tag{7}$$

Subsequently Amado and Woloshyn rederived [7], using a diagrammatic method and singularity analysis, the form factor

$$F(q)=\int dy\ e^{iqy}\rho(y)=A\prod_{n=1}^{A-1}\left[1+\left(\frac{q}{2n\lambda(A-1)}\right)^2\right]^{-1}. \tag{8}$$

Using the same technique they also derived [8] the momentum distribution for this model. As was noted earlier (see, e.g., [10], and references therein) the form factor of a bound system has a $[v(q)/q^2]^{A-1}$ asymptotic behavior[1] for $q\to\infty$. On the other hand, the asymptotic behavior of the momentum distribution [7] is given by $n(q)\to[v(q)/q^2]^2$. This means that for $q\to\infty$ the momentum distribution is dominated by two-particle correlations, whereas for the form factor only those configurations in which all particles take part in correlations are important.

III. ONE-BODY DENSITY MATRIX

In this section we want to show that not only the density and the momentum distribution but also the bound-state overlap function can be obtained from the full one-body density matrix [defined through Eqs. (A11), (A12)].

The OBDM can be calculated exactly in the model of Sec. II, by similar techniques as the ones used in [6–8]. Since it is a function of two independent variables, the derivation is more complicated than that of the form factor or momentum distribution. As it is also quite lenghty we refer to Appendix B for the used method and only state here the final result:

$$\widetilde{N}(y,a)=2\lambda(A-1)e^{-\frac{\lambda}{2}(A^2-1)|a|}\left(\sum_{n=1}^{A-1}e^{-2n\lambda(A-1)|y|}\sum_{m=-(A-1)}^{\overline{A-1}}e^{\frac{\lambda}{2}m(m-2n)|a|}(n-m)F_n^{(A)}+\sum_{m=1,2}^{\overline{A-1}}\theta(m|a|-2(A-1)|y|)\right.$$
$$\left.\times\sum_{n=-(A-1)}^{A-1}e^{2n\lambda(A-1)|y|}e^{\frac{\lambda}{2}m(m-2n)|a|}(n-m)F_n^{(A)}\right). \tag{9}$$

In this expression $\overline{\Sigma}$ denotes a summation over even (odd) numbers if A is odd (even). We checked that the diagonal of the OBDM, $N(y_A,y_A)=\widetilde{N}(y,a=0)$, reduces to the expression (4) for the density $\rho(y)$.

In Ref. [4] it was shown that the overlap function of bound eigenstates in the $(A-1)$-particle system can be obtained by examining the asymptotic behavior of the OBDM. This was based on the decomposition (A20) of the OBDM into the set of overlap functions, and exploiting the fact that the overlap functions corresponding to the $(A-1)$-particle eigenstates with the lowest energy have the weakest exponential decay [see Eq. (A9)].

Specifying to the present model we have only one bound $(A-1)$-particle eigenstate and its overlap function $\phi_{0(A-1)}$ is given by

$$\phi_{0(A-1)}(y'_A)=C'\lim_{y_A\to+\infty}N(y_A,y'_A)\exp\left(y_A\sqrt{2m\frac{A-1}{A}(E_{0(A-1)}-E_{0(A)})}\right)=C'\lim_{y_A\to+\infty}N(y_A,y'_A)\exp[\lambda(A-1)y_A]. \tag{10}$$

[1]The Fourier transform $v(q)$ of the two-body potential is just a constant in this schematic model.

The constant C' can be determined by considering also the limit $y'_A \to +\infty$ in Eq. (10), leading to

$$|C'|^{-2} = \lim_{y \to +\infty} \rho(y) \exp[2\lambda(A-1)y]. \tag{11}$$

In order to establish the asymptotic behavior of the OBDM in this model we take the limit $y_A \to +\infty$ in Eq. (9). This means we can substitute $|a| = y_A - y'_A$ and $|y| = \frac{1}{2}(y_A + y'_A)$ in (9). By inspection it is seen that in the first term of Eq. (9) the dominant exponential in y_A comes from $m = -(A-1)$. The argument of the step function in the second term of Eq. (9) becomes in the limit

$$\theta(m|a| - 2(A-1)|y|) = \theta([m-(A-1)]y_A - [m+(A-1)]y'_A) \to \delta_{m,A-1}\theta(-y'_A), \tag{12}$$

and only $m = A-1$ survives. Therefore the asymptotic behavior of the OBDM is given by

$$N(y_A, y'_A) \to 2\lambda(A-1)e^{-\lambda(A-1)y_A}\left(\sum_{n=1}^{A-1} e^{-\lambda(A-1)(2n-1)y'_A}(A-1+n)F_n^{(A)} - \theta(-y'_A) \right.$$
$$\left. \times \sum_{n=-(A-1)}^{A-1} e^{-\lambda(A-1)(2n-1)y'_A}(A-1+n)F_n^{(A)} \right). \tag{13}$$

The right-hand side of Eq. (13) is seen to be an even function in y'_A. This is expected since the ground-state to ground-state overlap function should have even parity. Using Eqs. (4,11) it follows that $|C'|^{-1} = (A-1)\sqrt{2\lambda}$.

The final result for the overlap function obtained through the OBDM with Eq. (10) is then given by

$$\phi_{0(A-1)}(y) = \sqrt{2\lambda} \sum_{n=1}^{A-1} e^{-\lambda(A-1)(2n-1)|y|}(A+n-1)F_n^{(A)}. \tag{14}$$

A direct calculation of the overlap function starting from Eq. (A7) can also be performed (see Appendix B), and yields exactly the same result. This confirms the properties derived in [4].

The spectroscopic factor of the bound-state overlap function,

$$S_{0(A-1)} = \int dy |\phi_{0(A-1)}(y)|^2, \tag{15}$$

is a measure for the degree of correlation in the system; i.e., $S_{0(A-1)} = A$ means no correlations. It is independent of λ. The fact that the strength of the interaction does not influence $S_{0(A-1)}$ is a less realistic feature of this simple model in which the wave functions contain only one dimensional parameter λ. We find that the system is only weakly correlated, with e.g., $(1/A)S_{0(A-1)} = 0.938$, 0.970, 0.997, for $A = 3$, 10, 100, respectively.

In Fig. 1 we compare the exact one-body density of the system with two approximations (the Hartree approximation and the contribution of the bound-state overlap function). As observed in [8], the spatial extent of the density decreases with $1/A$ for this nonsaturating system. Therefore it is convenient to plot the density $\rho(y)$ as a function of $A\lambda y$, in order to compare the results for different particle number.

It is seen that for all A the mean-field approximation gives too much central density and too little density in the tail. However, because the system is only weakly correlated [especially for fairly large A; see Eq. (15)], the mean field is an extremely good approximation to the density for all but the lightest systems. As expected the contribution from the bound-state overlap function reproduces the tail region of the density. This means that the contribution of the continuum-state overlap functions, which represent the possibility of n-particle emission ($n \geq 2$) from the target, is strongly localized in the center and of shorter range than the density itself. On the whole it is virtually impossible to distinguish on the basis of the one-body density between the system subject to the mean field (one-body forces) and the full system interacting through two-body forces.

We also obtained the natural orbitals of the system by direct numerical diagonalization of the OBDM, Eq. (9). As an example we discuss the natural basis for particle number $A = 10$. The nodeless orbital with even parity, which corresponds to the Bose condensate, has an occupation number $N = 9.927$. The remaining orbitals, of both even and odd parity, have much smaller occupation numbers which are smoothly decreasing with the number of nodes of the orbital. In Fig. 2 the largest occupation numbers are shown. In this model the occupation numbers of odd and even parity orbitals with the same number of nodes are rapidly converging to a common value.

The shapes of the natural orbitals are given in Fig. 3. In the upper panel the mean field, overlap, and natural orbital of the condensate are compared. The overlap and natural orbital are very similar, whereas the mean-field wave function is more pronounced in the center and less in the tail region. Some of the other natural orbitals are shown in the middle and lower panels. All natural orbitals are localized in the same region as the density $\rho(y)$, and the increasing number of nodes is confined within this region. This is qualitatively the same behavior of the natural basis as was found in a variational Monte Carlo calculation [11] of finite drops of ^{4}He atoms.

In Fig. 4 the asymptotic behavior of the natural orbitals in coordinate space is shown. In agreement with the results in [4], all the even-parity natural orbitals have the same expo-

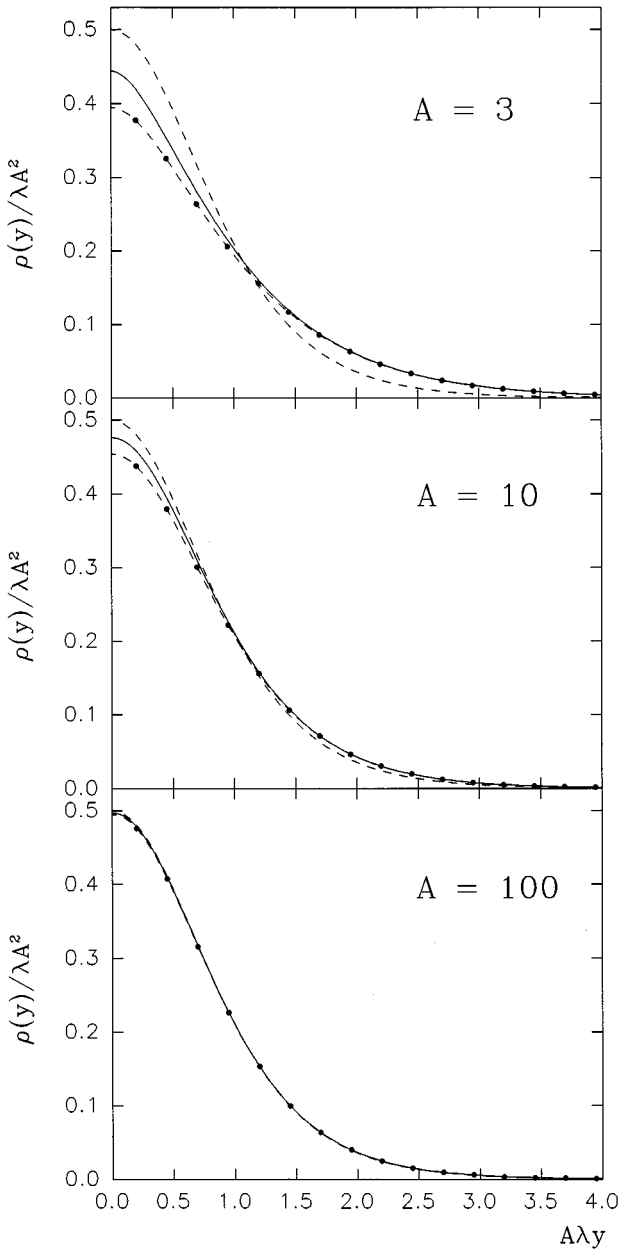

FIG. 1. One-body density for three values of the particle number A. Solid line: total density $\rho(y)$ [see Eq. (4)]. Dashed line: Hartree approximation $\rho^H(y)$ [see Eq. (7)]. Dashed line with dots: contribution of the bound-state overlap function $|\phi_{0(A-1)}(y)|^2$ [see Eq. (14)] to the density.

nential decay as the bound-state overlap function, since they have a nonvanishing overlap with the latter. The odd-parity natural orbitals, on the other hand, have a faster decay, which also seems to be universal.

IV. MOMENTUM-SPACE REPRESENTATION

Here we will focus on the high-momentum behavior of the momentum distribution, overlap functions, and natural orbitals.

The momentum distribution, defined through Eq. (A15), can be easily extracted from the OBDM, by means of Eq. (A14). We find

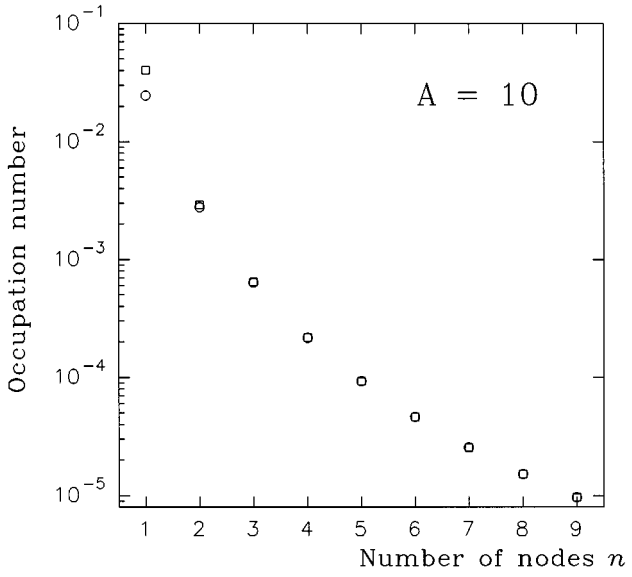

FIG. 2. Occupation number of the most occupied natural orbitals of even (squares) and odd (circles) parity, for particle number $A=10$. The occupation number of the nodeless natural orbital ($N=9.927$) is not shown in the figure.

$$n(q)=\frac{2}{\pi\lambda}\left[\sum_{m=1,2}^{A-1}\left(\frac{\alpha_m-m^2}{(q/\lambda)^2+\alpha_m^2}+\frac{2m^2\alpha_m^2}{[(q/\lambda)^2+\alpha_m^2]^2}\right)+\frac{1}{2}\delta(A\ \text{odd})\frac{\alpha_0}{(q/\lambda)^2+\alpha_0^2}\right], \tag{16}$$

with $\alpha_m=A^2-1-m^2$. The last term in (16) only contributes for A odd. We have also checked that Eq. (16) agrees with the expression for the momentum distribution in [8].

To establish the behavior of the momentum distribution (16) for $q\to\infty$ we first note that the coefficient $\tilde{C}_2$ of the asymptotic q^{-2} term,

$$\tilde{C}_2=\sum_{m=1,2}^{A-1}(\alpha_m-m^2)+\frac{1}{2}\delta(A\ \text{odd})\alpha_0, \tag{17}$$

vanishes for all A, as can be easily verified. The coefficient $\tilde{C}_4$ of the next q^{-4} term,

$$\tilde{C}_4=\sum_{m=1,2}^{A-1}(3m^2\alpha_m^2-\alpha_m^3)-\frac{1}{2}\delta(A\ \text{odd})\alpha_0^3, \tag{18}$$

does not vanish, however, and explicit calculation yields the desired asymptotic behavior of the momentum distribution

$$n(q)\to\frac{2}{\pi}\frac{1}{3}\lambda^3A(A^2-1)q^{-4}, \tag{19}$$

which corresponds to the $[v(q)/q^2]^2$ behavior, mentioned in Sec. II.

The exact expression for the momentum distribution is to be compared with the mean-field (Hartree) approximation [see Eq. (6)].

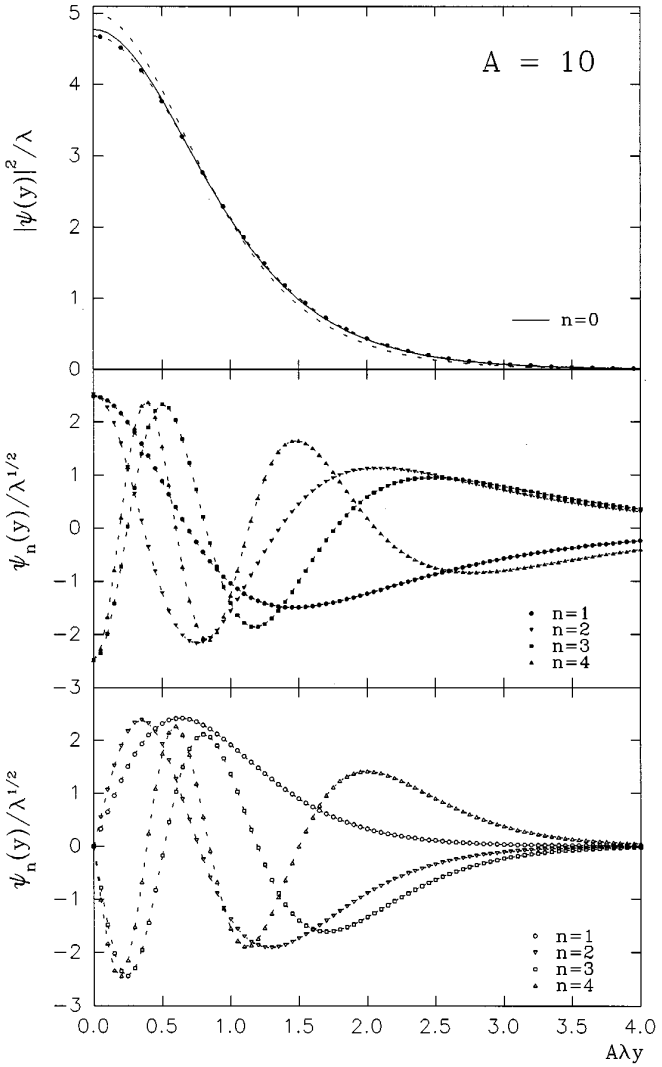

FIG. 3. Natural orbitals in coordinate space for particle number $A=10$. All wave functions are normalized to unity. Upper panel: comparison of the condensate natural orbital (solid line), the mean-field single-particle wave function (dashed line), and the overlap function (dashed line with dots). Middle (lower) panel: the four most occupied noncondensate natural orbitals with even (odd) parity.

$$n^H(q)=\frac{\pi}{4\lambda}\frac{1}{\cosh^2\left(\frac{\pi q}{2\lambda A}\right)}, \tag{20}$$

which has an exponential asymptotic behavior.

Finally we need the bound-state overlap function in momentum space. From Eqs. (A7), (A14) we get

$$\phi_{0(A-1)}(q) = \frac{2(A-1)}{\sqrt{\pi\lambda}}\sum_{k=1}^{A-1} F_k^{(A)}\frac{(2k-1)(A+k-1)}{(q/\lambda)^2+(A-1)^2(2k-1)^2}. \tag{21}$$

It can be shown that (21) can be rewritten in a similar form as the form factor [see Eq. (8)],

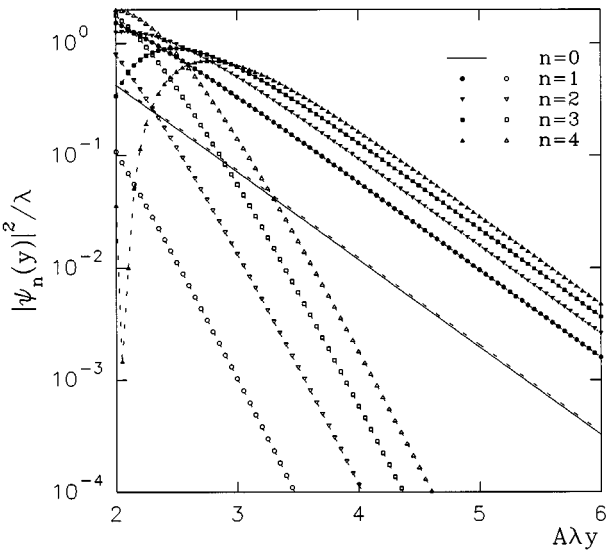

FIG. 4. Asymptotic behavior in coordinate space of the natural orbitals shown in Fig. 3. Solid line: natural orbital of the condensate. Solid (open) symbols: noncondensate natural orbitals with even (odd) parity. Dashed line: overlap function.

$$\phi_{0(A-1)}(q) = \frac{1}{\sqrt{\pi\lambda}}\frac{1}{2(A-1)}\prod_{k=1}^{A-1}\frac{[2k(A-1)]^2}{(q/\lambda)^2+(A-1)^2(2k-1)^2}, \tag{22}$$

leading to the asymptotic behavior

$$\phi_{0(A-1)}(q)\rightarrow\sqrt{\frac{\lambda}{\pi}}[2\lambda(A-1)]^{2A-3)}[(A-1)!]^2 q^{-2(A-1)}. \tag{23}$$

If this result is generalized to arbitrary many-body systems, one concludes that the asymptotic behavior of bound-state overlap functions is given by $[v(q)/q^2]^{A-1}$. This is not surprising since, just as is the case with the form factor, a large momentum kick has to be distributed over all particles when the residual system remains bound.

For $A=3$, Eq. (23) agrees with the $q\rightarrow\infty$ limit proposed in [12] for the spectral function of the three-nucleon system at fixed energy. The model in [12] also predicts for general A an approximate decomposition of the spectral function as a sum over contributions of j-particle correlations $(j=2,\ldots,A)$. It is interesting to note that this can be obtained from the product representation in Eq. (22) by approximating each factor

$$\frac{1}{(q/\lambda)^2+z^2}$$

by

$$\frac{\theta((q/\lambda)^2-z^2)}{(q/\lambda)^2}+\frac{\theta(z^2-(q/\lambda)^2)}{z^2}.$$

In Fig. 5 the exact momentum distribution, the Hartree approximation, and the contribution of the bound-state overlap function are compared. It is convenient to plot these

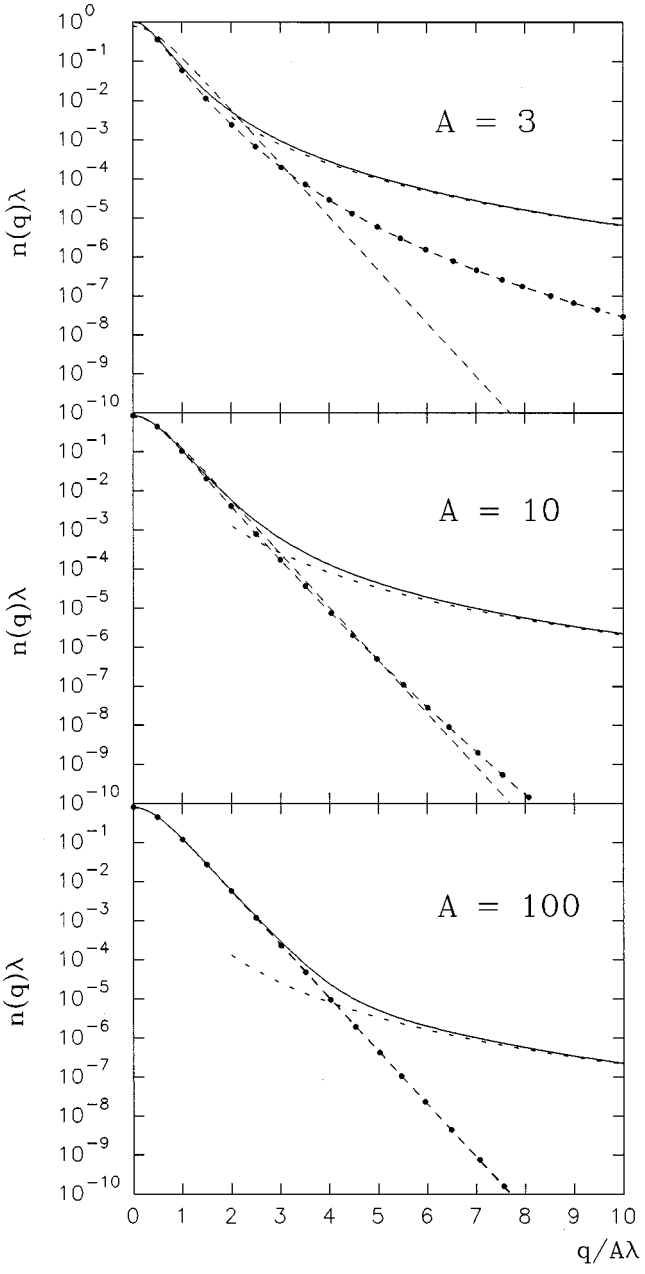

FIG. 5. Momentum distribution for three values of the particle number A. Solid line: total $n(q)$ [see Eq. (16)]. Dashed line: Hartree approximation $n^H(q)$ [see Eq. (20)]. Dashed line with dots: contribution of the bound-state overlap function $|\phi_{0(A-1)}(q)|^2$ [see Eq. (21)] to the momentum distribution. The short-dashed line is the asymptotic expression (19) for the total momentum distribution.

quantities as a function of $q/A\lambda$, since the extent of this nonsaturating system in momentum space increases linearly with A. The range of validity of the Hartree approximation and of the asymptotic expressions is shown in Fig. 6.

One observes from Fig. 5 that the Hartree solution provides a good approximation only for small q; as can be seen from Fig. 6 the range of validity is slowly increasing with A. At large momentum the two-body forces lead to an enhancement (by orders of magnitude) over the mean-field approximation. The point at which the power-law asymptotic regime of Eq. (19) is reached also has a very weak A dependence.

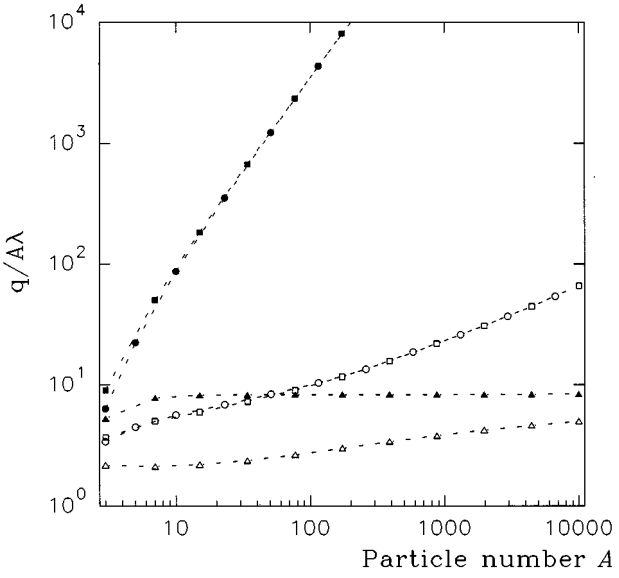

FIG. 6. The A dependence of the momentum value at which the exact expression for the momentum distribution (triangles), overlap function (circles), and form factor (squares) starts to deviate substantially from the power-law asymptotic behaviour and from the mean-field prediction. Solid symbols: q value beyond which the exact expression deviates by less than 10% from the asymptotic behavior. Open symbols: q value beyond which the exact expression is enhanced by more than 10% over the mean-field prediction.

The contribution of the bound-state overlap function behaves quite differently. It falls off much faster than the total momentum distribution, and although it is a rational function of q^2, it follows the exponential decay of the mean-field distribution up to quite large momenta, well beyond the point at which the total momentum distribution starts to deviate from the mean-field approximation. This means that the enhancement of the total momentum distribution over the mean field comes from n-particle emission channels ($n \geqslant 2$) which have a nonvanishing single-particle overlap with the ground state of the correlated system. The neglect of the recoil of the $(A-1)$ system in the Hartree calculation is not important for this enhancement.

The range in which the bound-state contribution is well approximated by the mean-field result rapidly increases with A; this is also the case for the point at which the power-law asymptotic regime of Eq. (19) is reached. One may observe from Fig. 6 that the overlap function and the form factor behave almost identically in this respect.

The natural orbitals in momentum space are shown in Fig. 7 for the case of particle number $A=10$. In the upper panel the natural orbital corresponding to the condensate is compared with the overlap function and the mean-field single-particle wave function; the natural orbital is closer to the overlap function. In the middle and lower panels some of the other natural orbitals are shown. The orbitals in momentum space have the same number of nodes as in coordinate space. They extend to larger momenta as the occupation number decreases (or the number of nodes increases).

In Fig. 8 we show separately the contribution to the total momentum distribution of the natural orbital of the condensate and of the most occupied other orbitals. The natural

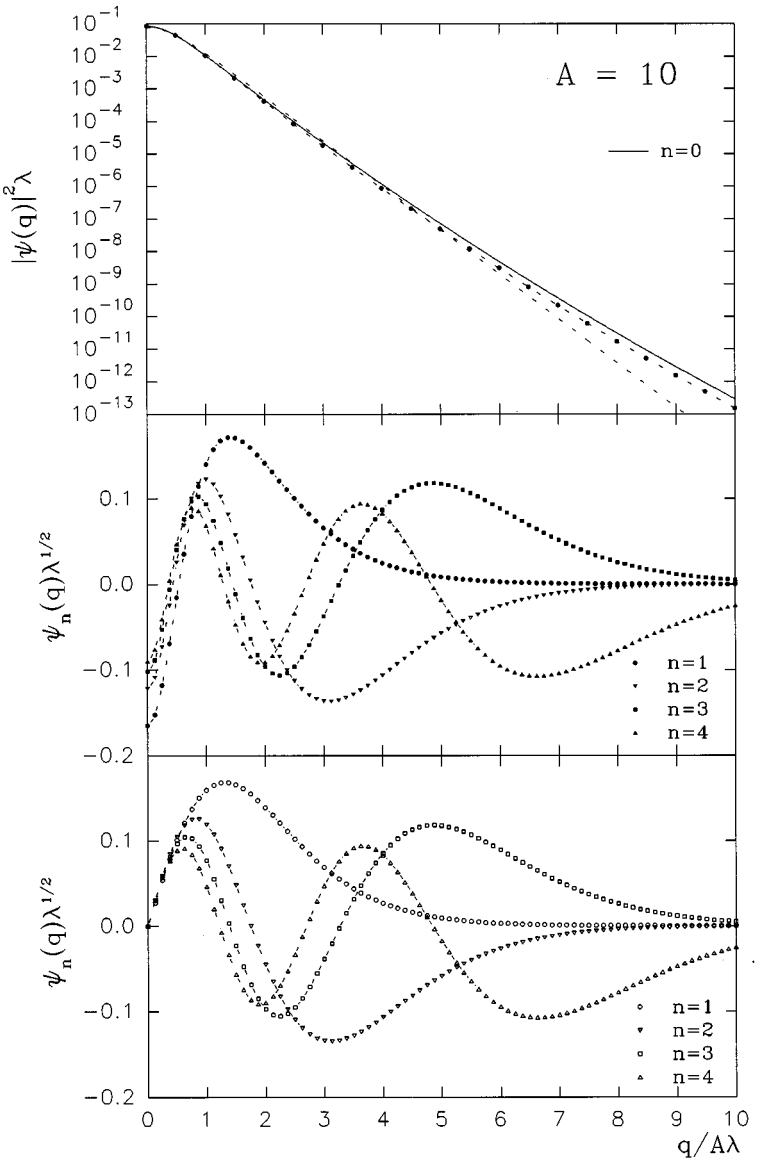

FIG. 7. Natural orbitals in momentum space for particle number $A=10$. All wave functions are normalized to unity. Upper panel: comparison of the condensate natural orbital (solid line), the mean-field single-particle wave function (dashed line), and the overlap function (dashed line with dots). Middle (lower) panel: the four most occupied noncondensate natural orbitals with even (odd) parity.

orbital of the condensate describes perfectly the small-q region of the momentum distribution. At larger q the momentum distribution is dominated by the noncondensate natural orbitals. In this model the natural orbitals of odd and even parity with the same number of nodes converge for large momenta. Since their occupation numbers also converge to a common value, the even and odd noncondensate natural orbitals contribute equally to the momentum distribution at large momenta.

V. SUMMARY AND CONCLUSION

In this paper we studied the single-particle properties of an exactly solvable schematic model, consisting of a system of spinless bosons interacting through delta-function potentials.

We examined the role of the overlap functions corresponding to bound and to continuum $(A-1)$-particle eigenstates. In r space the latter only contribute to the central density and fall of more quickly than the bound-state overlap functions, which describe the tail of the density. In q space the continuum-state overlap functions, which represent the possibility of n-particle emission ($n\geqslant 2$) from the correlated A-particle ground state, are responsible for the enhancement of the momentum distribution over the mean-field approximation at large momenta.

In this enhancement region the contribution of the bound-state overlap function to the momentum distribution is described accurately by the mean-field result for not too small A. Only at much larger momenta does the recoil of the $(A-1)$ system come into play and does the bound-state overlap function reach its inverse-power-law asymptotic behavior.

Although the model we discussed is quite schematic, it contains the essential many-body correlations in a system interacting through short-range forces, and many of its features should remain valid in the real world. Applied to the nuclear system, Fermi statistics would of course drastically affect the small-q region of the momentum distribution in the formation of a Fermi sea instead of the $q=0$ condensate, but the separation in a small-q region described by a mean field and the high-momentum region induced by two-body corre-

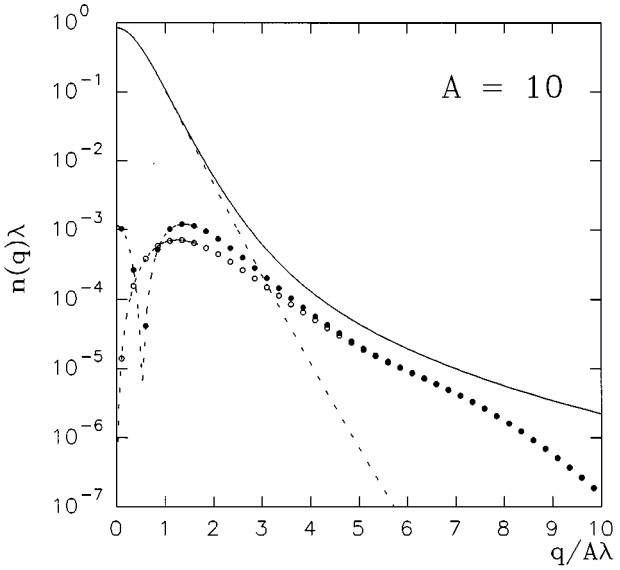

FIG. 8. Contribution to the momentum distribution $n(q)$ (solid line) of the natural orbital of the condensate (dashed line) and of the four most occupied noncondensate natural orbitals of even parity (solid circles) and odd parity (open circles), for particle number $A=10$.

lations should remain valid. Pauli blocking effects also lead to a faster fall off of the nuclear wave functions for large momenta, and in a three-dimensional system logarithmic corrections to the dominant inverse-power-law asymptotic behavior appear [10,8]. Finally the high-momentum tail will be modulated by a realistic NN interaction $v(q)$, which has strong short-range repulsion and a tensor component. This would lead to a stronger high-momentum enhancement.

The behavior of the bound-state overlap functions in q space is in agreement with many-body calculations using Green function perturbation theory [2] or the local density approximation [3]. On the other hand a recent $(e,e'p)$ experiment on ^{208}Pb, [13] in which the missing-momentum region 300–500 MeV/c of the valence hole overlap functions was probed, showed a large enhancement of the momentum distribution over the standard Woods-Saxon one. It was suggested in [3,13] that this may be due to the surface degrees of freedom in a finite system if strongly collective surface vibrational modes are present. Such surface effects were not taken into account in [2] or in the pure LDA calculation in [3], and are evidently absent in the one-dimensional model discussed in this paper.

The considered model is an example of a quantum many-body system interacting through short-range forces. Such systems have certain universal properties; e.g., it was shown recently [4] that it is possible to derive the bound-state overlap functions, spectroscopic factors, and separation energies from the one-body density matrix. In this paper we confirmed this property by an explicit construction in an exactly solvable model.

ACKNOWLEDGMENTS

This work is part of the research program of the foundation for Fundamental Research of Matter (FOM), which is financially supported by the Netherlands Organisation for Advancement of Pure Research (NWO).

APPENDIX A: CONVENTIONS

Several conventions are possible for single-particle quantities in self-bound many-body systems, when translational invariance of the wave functions is taken into account. Therefore we will state explicitly the definitions we have adopted in this paper.

The coordinate space wave functions that describe the relative motion are translationally invariant, $\Psi(x_1,\ldots,x_A)=\Psi(x_1+X,\ldots,x_A+X)$. Orthogonality and completeness of the eigenstates of the intrinsic hamiltonian can then be expressed as[2]

$$\int \left(\prod_{i=1}^{A} dx_i\right) \Psi_\mu^*(x_1,\ldots,x_A)\Psi_\nu(x_1,\ldots,x_A)\,\delta\left(\frac{1}{A}\sum_{i=1}^{A} x_i\right) = \delta_{\mu,\nu}, \tag{A1}$$

$$\sum_{\nu(A)} \Psi_\nu(x_1,\ldots,x_A)\Psi_\nu^*(x_1',\ldots,x_A') = \int dX \prod_{i=1}^{A} \delta(x_i-x_i'+X). \tag{A2}$$

Similarly the relative wave functions in momentum space obey

$$\int \left(\prod_{i=1}^{A} dq_i\right) \Psi_\mu^*(q_1,\ldots,q_A)\Psi_\nu(q_1,\ldots,q_A)\,2\pi\delta \times\left(\sum_{i=1}^{A} q_i\right) = \delta_{\mu,\nu}, \tag{A3}$$

$$\sum_{\nu(A)} \Psi_\nu(q_1,\ldots,q_A)\Psi_\nu^*(q_1',\ldots,q_A') = \frac{1}{2\pi}\int dK \prod_{i=1}^{A} \delta\left(q_i-q_i'+\frac{K}{A}\right), \tag{A4}$$

and momentum and coordinate space wave functions are related by

$$\Psi(q_1,\ldots,q_A)=\frac{1}{(2\pi)^{A/2}}\int \left(\prod_{i=1}^{A} dx_i\right)\Psi(x_1,\ldots,x_A) \times\exp\left(-i\sum_{i=1}^{A} q_i x_i\right)\delta\left(\frac{1}{A}\sum_{i=1}^{A} x_i\right). \tag{A5}$$

For the overlap functions ϕ_ν between the ground state of the A-particle system and the $(A-1)$-particle eigenstates we adopt the following definition in momentum space:

[2]The summation over eigenstates in Eqs. (A2), (A4), (A10) must be understood to include integrations over the unbound eigenstates in the different continuum channels.

$$\phi_\nu(q_A)=\sqrt{A}\int\left(\prod_{i=1}^{A-1}dq_i\right)\Psi^*_{\nu(A-1)}(q_1,\ldots,q_{A-1})\times\Psi_{0(A)}(q_1,\ldots,q_A)2\pi\delta\left(\sum_{i=1}^{A}q_i\right). \tag{A6}$$

This corresponds to the amplitude for extracting a particle with momentum q_A from the ground state $\Psi_{0(A)}$ of the target in rest, ending up in the eigenstate $\Psi_{\nu(A-1)}$ of the residual system, and as such the convention of Eq. (A6) is most closely related to the description of one-particle knockout reactions.

The overlap function in coordinate space then follows by Fourier transforming,

$$\begin{aligned}\phi_\nu(x_A)&=\frac{1}{(2\pi)^{1/2}}\int dq_A e^{iq_Ax_A}\phi_\nu(q_A)\\&=\sqrt{A}\int\left(\prod_{i=1}^{A-1}dx_i\right)\Psi^*_{\nu(A-1)}(x_1,\ldots,x_{A-1})\times\Psi_{0(A)}(x_1,\ldots,x_A)\,\delta\left(\frac{1}{A-1}\sum_{i=1}^{A-1}x_i\right).\end{aligned} \tag{A7}$$

An equivalent expression (which will be used in Appendix B) reads as

$$\phi_\nu(y)=\sqrt{A}\int\left(\prod_{i=1}^{A-1}dx_i\right)\Psi^*_{\nu(A-1)}(x_1,\ldots,x_{A-1})\times\Psi_{0(A)}(x_1,\ldots,x_{A-1},0)\,\delta\left(y+\frac{1}{A-1}\sum_{i=1}^{A-1}x_i\right). \tag{A8}$$

If the forces between the particles are of sufficiently short range, the asymptotic behavior of the overlap functions is given by [14]

$$\phi_{\nu(A-1)}(y)\rightarrow\frac{1}{C'}\exp\left(-|y|\sqrt{2m\frac{A-1}{A}(E_{\nu(A-1)}-E_{0(A)})}\right). \tag{A9}$$

Equation (A9) is the generalization of Eq. (10) in [4] when center-of-mass motion of the residual system is taken into account.

The OBDM is decomposed in terms of the overlap functions as

$$N(y_A,y'_A)=\sum_{\nu(A-1)}\phi^*_\nu(y'_A)\phi_\nu(y_A). \tag{A10}$$

Using the completeness relation (A2) this is equivalent to

$$N(y_A,y'_A)=A\int\left(\prod_{i=1}^{A-1}dx_i\right)\Psi^*_{0(A)}(x_1,\ldots,x_{A-1},y'_A)\times\Psi_{0(A)}(x_1,\ldots,x_{A-1},y_A)\,\delta\left(\frac{1}{A-1}\sum_{i=1}^{A-1}x_i\right). \tag{A11}$$

It is sometimes more convenient to introduce the relative and center-of-mass coordinates $a=y_A-y'_A$ and $y=\frac{1}{2}(y_A+y'_A)$, in terms of which the OBDM becomes

$$\begin{aligned}\widetilde{N}(y,a)&=N(y_A,y'_A)\\&=A\int\left(\prod_{i=1}^{A-1}dx_i\right)\Psi^*_{0(A)}\left(x_1,\ldots,x_{A-1},-\frac{a}{2}\right)\times\Psi_{0(A)}\left(x_1,\ldots,x_{A-1},\frac{a}{2}\right)\delta\left(y+\frac{1}{A-1}\sum_{i=1}^{A-1}x_i\right).\end{aligned} \tag{A12}$$

The density $\rho(y)$ is defined as the diagonal of the OBDM,

$$\begin{aligned}\rho(y)&=N(y,y)=\widetilde{N}(y,a=0)\\&=A\int\left(\prod_{i=1}^{A-1}dx_i\right)|\Psi_{0(A)}(x_1,\ldots,x_{A-1},y)|^2\times\delta\left(\frac{1}{A-1}\sum_{i=1}^{A-1}x_i\right),\end{aligned} \tag{A13}$$

and represents the probability of finding a particle at distance y of the center-of-mass of the $(A-1)$ other particles.

The momentum distribution $n(q)$ can be obtained from the OBDM with the relation

$$n(q)=\frac{1}{2\pi}\int da\ e^{-iqa}\int dy\ \widetilde{N}(y,a). \tag{A14}$$

Using Eq. (A5) this can be rewritten in terms of the ground-state wave function in momentum space as

$$n(q)=A\int\left(\prod_{i=1}^{A-1}dq_i\right)|\Psi_{0(A)}(q_1,\ldots,q_{A-1},q)|^2 2\pi\delta\times\left(q+\sum_{i=1}^{A-1}q_i\right), \tag{A15}$$

and so $n(q)$ represents the probability of finding a particle with momentum q if the total system is in rest.

In Eqs. (A13), (A15) both $\rho(y)$ and $n(q)$ are normalized to the number of particles,

$$A=\int dy\ \rho(y)=\int dq\ n(q). \tag{A16}$$

APPENDIX B: CALCULATION OF THE OBDM AND OVERLAP FUNCTION

Upon substitution of the expression (3) for the many-body wave function into the defining relations (A12) and (A8) we get

$$\widetilde{N}(y,a)=AC_A^2\int\left(\prod_{i=1}^{A-1}dx_i\right)\exp\left(-2\lambda\sum_{i<j=1}^{A-1}|x_i-x_j|\right)\times\exp\left(-\lambda\sum_{i=1}^{A-1}\left\{\left|x_i-\frac{a}{2}\right|+\left|x_i+\frac{a}{2}\right|\right\}\right)\times\delta\left(y+\frac{1}{A-1}\sum_{i=1}^{A-1}x_i\right), \tag{B1}$$

$$\phi_0(y)=\sqrt{A}C_AC_{A-1}\int\left(\prod_{i=1}^{A-1}dx_i\right)\exp\left(-2\lambda\sum_{i<j=1}^{A-1}|x_i-x_j|\right)\times\exp\left(-\lambda\sum_{i=1}^{A-1}|x_i|\right)\delta\left(y+\frac{1}{A-1}\sum_{i=1}^{A-1}x_i\right). \tag{B2}$$

The absolute-value functions containing differences of internal integration variables x_i can be simply evaluated by considering one ordering $-\infty<x_1<\cdots<x_{A-1}<+\infty$ and using the symmetry of the integrand under permutations of the x_i. In order to resolve the absolute-value functions related to the external points we split the interval for the internal x_i integrations in Eqs. (B1), (B2) into four distinct regions $[-\infty,-a/2],[-a/2,0],[0,+a/2],[+a/2,+\infty]$ for the OBDM, and into two regions $[-\infty,0],[0,+\infty]$ for the overlap function. The total integration volume in Eqs. (B1), (B2) is then obtained by summing over all the possible partitions of $(A-1)$ particles into the distinct integration regions; e.g., for $\tilde{N}(y,a)$ we have

$$\begin{aligned}\int\left(\prod_{i=1}^{A-1}dx_i\right)&=(A-1)!\ {}_{(<)}\int_{-\infty}^{+\infty}\left(\prod_{i=1}^{A-1}dx_i\right)\\&=(A-1)!\sum_{\substack{l_1,l_2,l_3,l_4=0\\(l_1+l_2+l_3+l_4=A-1)}}^{A-1}{}_{(<)}\int_{-\infty}^{-a/2}\left(\prod_{i=1}^{l_1}dx_i\right)\\&\quad\times{}_{(<)}\int_{-a/2}^{0}\left(\prod_{i=l_1+1}^{l_1+l_2}dx_i\right){}_{(<)}\int_{0}^{a/2}\left(\prod_{i=l_1+l_2+1}^{l_1+l_2+l_3}dx_i\right){}_{(<)}\int_{a/2}^{+\infty}\left(\prod_{i=l_1+l_2+l_3+1}^{A-1}dx_i\right),\end{aligned} \tag{B3}$$

where we have introduced the notation

$${}_{(<)}\int_a^b\left(\prod_{i=1}^{N}dx_i\right)=\int_a^b dx_N\int_a^{x_N}dx_{N-1}\cdots\int_a^{x_2}dx_1. \tag{B4}$$

Likewise, for $\phi_0(y)$ we make a partition

$$\int\left(\prod_{i=1}^{A-1}dx_i\right)=(A-1)!\sum_{\substack{l_1,l_2=0\\(l_1+l_2=A-1)}}^{A-1}{}_{(<)}\int_{-\infty}^{0}\left(\prod_{i=1}^{l_1}dx_i\right){}_{(<)}\int_{0}^{+\infty}\left(\prod_{i=l_1+1}^{A-1}dx_i\right). \tag{B5}$$

Replacing the c.m. δ functions in the integrand by the Fourier expansion $[2\pi\delta(z)=\int dT\ \exp(iTz)]$ it is now possible to obtain an expression for Eqs. (B1)–(B2) in terms of generic integrals $G(a,b,\{C_i\})$, which are defined as $(a<b)$

$$G(a,b,\{C_j\})={}_{(<)}\int_a^b dx_1\cdots dx_N\exp\left(\sum_{j=1}^{N}C_jx_j\right). \tag{B6}$$

The G integral can be worked out in a straightforward but tedious way as

$$G(a,b,\{C_i\})=\sum_{m=0}^{N}(-1)^m\frac{\exp(bB_{(m)N-m})\exp(aA_{(m)m})}{(\Pi_{k=1}^{N-m}B_{(m)k})(\Pi_{k=1}^{m}A_{(m)k})}, \tag{B7}$$

with $A_{(m)k}=\Sigma_{j=1}^{k}C_{m-j+1}$ and $B_{(m)k}=\Sigma_{j=1}^{k}C_{m+j}$.

For the overlap function $\phi_0(y)$ this procedure leads to

$$\phi_0(y)=\widetilde{C}\sum_{\substack{l_1,l_2=0\\(l_1+l_2=A-1)}}^{A-1}\frac{1}{2\pi}\int dT\ \exp[-2iT\lambda(A-1)y]\times G(-\infty,0,\{C_j^{(1)}\})G(0,+\infty,\{C_j^{(2)}\}), \tag{B8}$$

with $\widetilde{C}=2\sqrt{A}(A-1)!(A-1)C_AC_{A-1}\lambda^{-(A-2)}$. The sets of coefficients $\{C_j^{(i)}\}$, with $i=1,2$ and $j=1,\ldots,l_i$ in Eq. (B8) are given by

$$C_j^{(1)}=2\left(-2j+A+\frac{1}{2}-iT\right),$$

$$C_j^{(2)}=2\left(-2j+l_2-l_1+\frac{1}{2}-iT\right). \tag{B9}$$

After working out the corresponding A and B coefficients one can easily write down, using Eq. (B7), the contributions of each G factor to the T integrand in Eq. (B8). We have

$$G(-\infty,0,\{C_j^{(1)}\})=\frac{1}{l_1!2^{l_1}\Pi_{k=1}^{l_1}(A-k-\frac{1}{2}-iT)}, \tag{B10}$$

and $G(0,+\infty,\{C_j^{(2)}\})$ follows from Eq. (B10) by taking the complex conjugate and interchanging $l_1 \leftrightarrow l_2$.

The integrand in Eq. (B8) is now seen to contain a product of $(A-1)$ simple poles, and the T integration is easily done by complex contour integration. Because of the factor $\exp[-2iT\lambda(A-1)y]$, the contour must be closed in the upper or lower half of the complex T plane depending on the sign of y. For $y<0$ one finds

$$\phi_0(y)=\theta(-y)\widetilde{C}\sum_{\substack{l_1,l_2=0\\(l_1+l_2=A-1)}}^{A-1}\sum_{k=1}^{l_2}\frac{(2A-2-k-l_1)!(-1)^{l_2+k}\,e^{2\lambda(A-1)(A-k-(1/2))y}}{(2A-2-k)!(k-1)!(l_2-k)!(A-1)!2^{A-1}}. \tag{B11}$$

One of the summations in Eq. (B11) can be eliminated using the combinatorial identity

$$\sum_{l=0}^{A-k}(-1)^l\binom{A-k}{l}\binom{A+l}{A-k}=(-1)^{A-k}, \tag{B12}$$

and the final result for ϕ_0 is

$$\phi_0(y)=\widetilde{C}\sum_{k=1}^{A-1}(-1)^{A-k+1}\frac{e^{-\lambda(A-1)(2A-2k-1)|y|}}{(k-1)!(2A-k-2)!2^{A-1}}, \tag{B13}$$

which corresponds to Eq. (14) in the text.

For the OBDM the strategy is the same but the algebra gets more involved. The expression in terms of G integrals is

$$\widetilde{N}(y,a)=\widetilde{C}\sum_{\substack{l_1,l_2,l_3,l_4=0\\(l_1+l_2+l_3+l_4=A-1)}}^{A-1}\frac{1}{2\pi}\int dT\,\exp[-iT\lambda(A-1)y]\exp[-(l_2+l_3)\lambda a]$$
$$\times G\left(-\infty,-\frac{\lambda a}{2},\{C_j^{(1)}\}\right)G\left(-\frac{\lambda a}{2},0,\{C_j^{(2)}\}\right)G\left(0,\frac{\lambda a}{2},\{C_j^{(3)}\}\right)G\left(\frac{\lambda a}{2},+\infty,\{C_j^{(4)}\}\right), \tag{B14}$$

with $\widetilde{C}=A!(A-1)C_A^2\lambda^{-(A-2)}$. The sets of coefficients $\{C_j^{(i)}\}$, with $i=1,\ldots,4$ and $j=1,\ldots,l_i$, in Eq. (B14) are given by

$$\begin{aligned}
&C_j^{(1)}=2(-2j+A+1-iT), \quad C_j^{(2)}=2(-2j-2l_1+A-iT),\\
&C_j^{(3)}=2(-2j+2l_3+2l_4-A+2-iT),\\
&C_j^{(4)}=2(-2j+2l_4-A+1-iT).
\end{aligned} \tag{B15}$$

The contribution of each G factor to the T integrand in Eq. (B14) is given by

$$G\left(-\infty,-\frac{\lambda a}{2},\{C_j^{(1)}\}\right)=\frac{\exp[-l_1\lambda(A-l_1-iT)a]}{l_1!2^{l_1}\Pi_{k=1}^{l_1}(A-k-iT)}, \tag{B16}$$

$$G\left(-\frac{\lambda a}{2},0,\{C_j^{(2)}\}\right)=\sum_{m=0}^{l_3}(-1)^m\frac{\exp[(l_3-m)(2l_4+l_3-A+1-m-iT)\lambda a]}{2^{l_3}m!(l_3-m)!\Pi_{k=1}^{l_3-m}(2l_3+2l_4-A+1-2m-k-iT)}$$
$$\times\frac{1}{\Pi_{k=1}^{m}(2l_3+2l_4-A+1-2m+k-iT)}, \tag{B17}$$

whereas $G(0,\lambda a/2,\{C_j^{(3)}\})$ and $G(\lambda a/2,+\infty,\{C_j^{(4)}\})$ follow from Eqs. (B17) and (B16) by complex conjugation and the interchange $l_1\leftrightarrow l_4, l_2\leftrightarrow l_3$. Again the T integral in Eq. (B14) can be worked out by contour integration. The resulting complicated sum can be simplified considerably by using combinatorial identities such as Eq. (B12), and leads finally to expression (9) for the full OBDM.

[1] A.E.L. Dieperink and P.K.A. de Witt Huberts, Annu. Rev. Nucl. Part. Sci. **40**, 239 (1990).
[2] H. Müther and W.H. Dickhoff, Phys. Rev. C **49**, R17 (1994).
[3] D. Van Neck, A.E.L. Dieperink, and E. Moya de Guerra, Phys. Rev. C **51**, 1800 (1995).
[4] D. Van Neck, M. Waroquier, and K. Heyde, Phys. Lett. B **314**, 255 (1993).
[5] J.B. McGuire, J. Math. Phys. **5**, 622 (1964).
[6] F. Calogero and A. Degasperis, Phys. Rev. A **11**, 265 (1975).
[7] R.D. Amado, Phys. Rev. C **14**, 1264 (1976); R.D. Amado and R.M. Woloshyn, Phys. Lett. **62B**, 253 (1976)
[8] R.D. Amado and R.M. Woloshyn, Phys. Rev. C **15**, 2200 (1977).
[9] A.N. Antonov, P.E. Hodgson, and I.Zh. Petkov, *Nucleon Momentum and Density Distributions in Nuclei* (Clarendon Press, Oxford, 1988); *Nucleon Correlations in Nuclei* (Springer, Berlin), 1993).
[10] I.M. Narodetsky, Yu.A. Simonov, and F. Palumbo, Phys. Lett. **58B**, 125 (1975).
[11] D.S. Lewart and V.R. Pandharipande, Phys. Rev. B **37**, 4950 (1988).
[12] L. Frankfurt and M. Strikman, Phys. Rep. **160**, 235 (1988).
[13] I. Bobeldijk *et al.*, Phys. Rev. Lett. **73**, 2684 (1994).
[14] J.M. Bang, F.G. Gareev, W.T. Pinkston, and J.S. Vaagen, Phys. Rep. **125**, 253 (1985).